The Seasonal Zonal Equatorial Undercurrent Strength variation with ENSO

Yanfeng Shao

University of Washington, Seattle, WA

School of Oceanography

Email: ys267@uw.edu

03/08/2024

Abstract:

The Equatorial Undercurrent (EUC) is an important current both physically and biologically. It is not only key to equatorial circulation but also closely related to primary production at the Equator. Seasonal variation of EUC is caused by the seasonality of the equatorial thermocline. This study retrieves in situ EUC velocity data using an ADCP from the TN427 cruise, traveling from 5°N to 5°S at 170°W in December and January, from 2023 - 2024. During the first crossing through equator, the maximum EUC velocity was measured to be 0.42 $\frac{m}{s}$ and mean EUC velocity was 0.02 $\frac{m}{s}$. Calculated transport equals to 10.77 Sverdrup. During the second crossing, the velocity is measured to be 0.59 m/s with 0.04 $\frac{m}{s}$ mean velocity. The transport for the second crossing was 14.78 Sverdrup. The maximum EUC velocity at the beginning of 2024 is much lower than the value in 2023, which was caused by the increase in upwelling during El Niño. According to the most recent ENSO SSTA indices of Niño 3.4 from NOAA State of Ocean Climate, the peak of Niño 3.4 index was in December 2023 and January 2024, followed by a decrease in Niño 3.4 index. Future prediction states that an increase of maximum EUC velocity will be observed within the next few months.

Plain language summary:

The Equatorial Undercurrent (EUC) is a significant oceanic feature that plays a crucial role in the context of El Niño and La Niña events. The EUC is a current that flows from west to east, which is opposite to the surface current at equator. The depth of EUC is normally from 50 m to 200 m at the equator. The EUC velocity is driven not only by the difference in sea surface height but also by upwelling, which can be reflected in the sea surface temperature. Therefore, the sea surface temperature difference between El Niño and La Niña years is important for predicting

EUC velocity, and we observed that the EUC velocity during El Niño is generally slower than the velocity during La Niña. In this study, real time EUC velocity data was collected at the equator during the expedition. Historical data was found on the NOAA TAO Array website and could also be used for comparison. The hypothesis is that the zonal EUC velocity will decrease and reach a lower value than that observed during the previous El Niño. The results show a lower EUC velocity compared to 2023, while the Niño index increases. However, to draw a reasonable conclusion, further data in March and April are required due to the seasonal variability of the EUC.

Introduction:

El Niño-Southern Oscillation (ENSO) is a climate pattern that alternates between El Niño and La Niña in the equatorial Pacific. During El Niño and La Niña, a sea surface temperature (SST) anomaly has been observed along the equator. The region emphasized in this paper is called Niño 3.4 (120°-170°W and 5°N-5°S), which is also the most used index for analyzing ENSO patterns. The SST difference between El Niño and La Niña is presented at the equator (Figure 1), where current strength is primarily driven by wind. The periodic cycle of winds, changes in atmospheric pressure, and sea surface temperatures (SSTs) in the equatorial Pacific is observed and believed to be the cause of ENSO. Previous studies have shown that strong zonal winds along the equator and meridional circulation are primary factors controlling the circulation of the equatorial Pacific Ocean (Peng, 1998). The wind at the equator is closely related to the complex water circulation, which is broadly reflected by the entire ENSO pattern, including changes in SST and current velocity. During El Niño, SST increases while Hadley cell circulation intensifies. The Hadley cell is a circulation pattern in the tropical region where wind rises at the equator and sinks at higher latitudes. This increase of SST gradient is causing easterly trade

winds to strengthen. Then, this trade winds' strength increases, driving Ekman transport in the eastern equatorial Pacific. The Ekman transport leads to upwelling and a decrease in SST, entering the La Niña cycle (Bjerknes, 1969). The ENSO index (ONI) (Figure 2) was introduced by NOAA to reflect the phase and strength of ENSO.

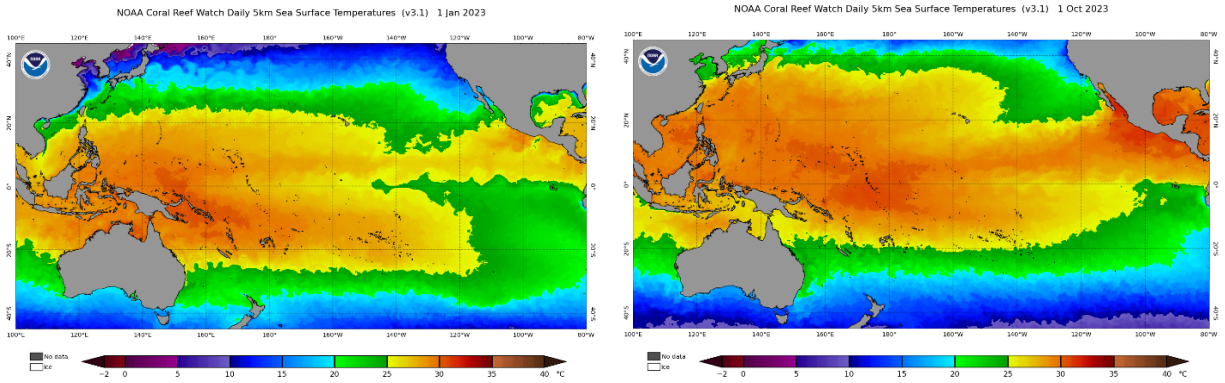

Figure 1. The La Niña (left) SST along the equator. Data was collected on 1 January 2023, which was at the valley of Multivariate ENSO index (Figure 2). The SST of El Niño (right) collected on 1 October 2023, when Multivariate ENSO index was positive and show increasing trend (NOAA, 2023).

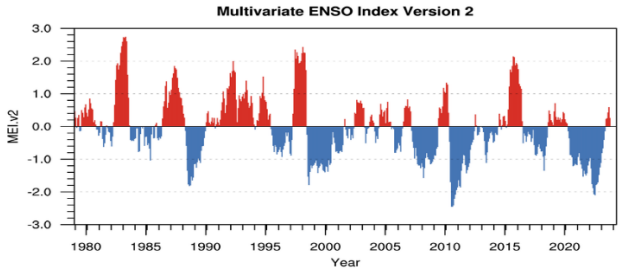

Figure 2. The ENSO Index represents the phase of ENSO with multiple atmospheric and oceanic indicators. The index above 0 represents El Niño and is positively related to the strength of it (Red). The index below 0 represents La Niña and negatively related to its strength (Blue) (NOAA, 2023) (https://www.ospo.noaa.gov/Products/ocean/sst/anomaly/).

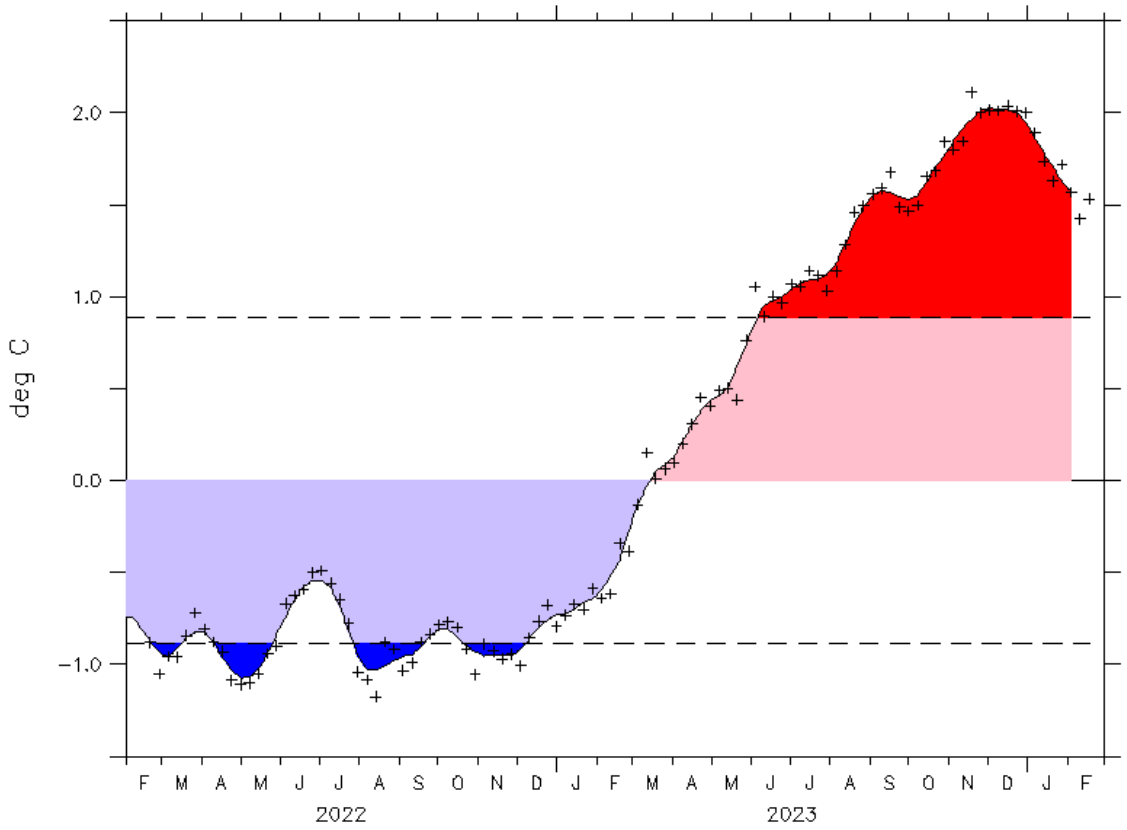

Figure 3. updated Niño 3.4 index till January 2024. Monthly averages are shown in plus sign and seasonal mean (three month) filtered index values are shown in shaded area. The uncertainty of this index is estimated to be 0.05835°C since 1982.

The ENSO index began to increase in December 2022 and reached its peak between December 2023 and January 2024 (https://stateoftheocean.osmc.noaa.gov/sur/pac/nino34.php). The expedition in this study (TN427) began in December 2023 and ended in January 2024, when El Niño in 2024 reaches its peak (Figure 3). The rate of increase of the ENSO index has been high

since December 2022 (Figure 3). El Niño conditions have emerged due to the atmospheric response to elevated temperatures in the tropical Pacific Ocean since March 2023. Projections indicate that El Niño is likely to persist throughout the winter, with a 56% probability of intensifying into a strong event at its peak. There is a high likelihood, approximately 84%, of it reaching at least a moderate level (Becker et al., 2023). According to a recent study by the NOAA Climate Prediction Team, there will be at least a "strong" El Niño event with a chance of more than 75% between November and January (≥ 1.5°C for the seasonal average in Niño-3.4). There is a 30% chance of a "historically strong" event appearing in the year 2024 (Climate Prediction Center Internet Team, 2023). Equatorial Undercurrent velocity data from 2015 to 2016 and 1997 to 1998 has been recorded on the NOAA Global Tropical Moored Buoy Array (https://www.pmel.noaa.gov/tao/drupal/disdel/). Previous study found EUC is located at depth of 50 to 150 meters and coincides with the depth of equatorial thermocline (Quintana et al., 2021; Johnson et al., 2002). Because the El Niño strength in Pacific has been increasing since December 2023, the data from TN413 cruise will be used for reference and comparison with data acquired from cruises from American Samoa.

The Equatorial Undercurrent is an important factor when studying circulation along the equator (Cromwell et al., 1954; Knauss, 1959). The Equatorial Undercurrent (EUC) is a subsurface (50 – 200 m) current that flows in an east-west direction along the equator. Th velocity of EUC normally reach 1.0 $\frac{m}{s}$ at its core and the transport is calculated to be approximately 30 to 40 Sv (Izumo. 2005). The EUC flows eastward primarily due to the direction and strength of the trade winds. The strength of the trade winds enhances during La Niña, causing more upwelling and a higher velocity of the EUC flowing eastward. The upwelling water flows towards the eastern pacific equatorial Pacific. Due to the Coriolis force generated by the spinning of the Earth, the

water on the surface diverged towards the subtropics in both North and South hemisphere (Gu and Philander 1997). During the El Niño phase of ENSO, trade winds weakened or reversed. This variation could be disrupted by the weakening or reversing trade winds, which would cause flattening of the thermocline (McPhaden, 1999). The weakening trade winds result in less upwelling, representing a weaker EUC velocity because of a lower water circulation. The strength of the zonal equatorial current is closely related to circulation at the equator, which can vary significantly depending on the phases of the ENSO event, as it is located on the equatorial thermocline (Johnson et al., 2002). Although measuring upwelling in the equatorial Pacific directly was challenging (Johnson & McPhaden, 2001), there are still methods that include chemical tracers (Quay, 1983) and calculations based on Ekman transport and geostrophic dynamics (Wyrtki, 1981). The Acoustic Doppler Current Profiler (ADCP) will be applied to obtain current velocity at each station. The ADCP is an instrument that measures current velocity over a range of depths using a more efficient and accurate method. It utilizes the Doppler effect, which refers to the change in frequency of a wave as an object travels through it, to calculate water current velocity. In 2001, around 70 moorings within the Tropical Atmosphere Ocean/Triangle Trans-Ocean Buoy Network (TAO/TRITON) Array were collecting data using ADCPs within the geographical range of 137°E to 95°W and 8°S to 8°N (McPhaden, 2001).

The EUC structure and strength are strongly driven by wind in the equatorial Pacific Ocean (Peng, 1998). However, EUC velocity is also influenced by upwelling in the same region, and the upwelling pattern can be reflected through the temperature-depth profile. The weaker zonal circulation and upwelling at the equator (Wyrtki, 1981) are not only important components of the overall circulation but also have a significant influence on global climate and biogeochemical cycles (Johnson & McPhaden, 2001). It is crucial to understand the current structure of the

equatorial Pacific and its upwelling pattern. Such circulation during ENSO events could be utilized for the construction of mathematical models and future predictions in both physical and biological oceanography.

Hypothesis

The R/V Thompson collected ADCP data during two crossings of the equator - one in Feb. 2023 as the equatorial Pacific was in a neutral phase and in Jan. 2024 as El Niño conditions were at their peak. The hypothesis of this study is that the strength of the EUC will have greatly increased between these two transects due to the decrease in strength of El Niño. The EUC velocity in the equatorial Pacific was approximately 70 cm/s slower in El Niño years than La Niña years (Figure 5). The underlying principle behind this phenomenon could be explained by the weakening of trades wind, there is less of a pressure gradient driving the EUC, therefore the EUC velocity is expected to be slower. (Figure 4).

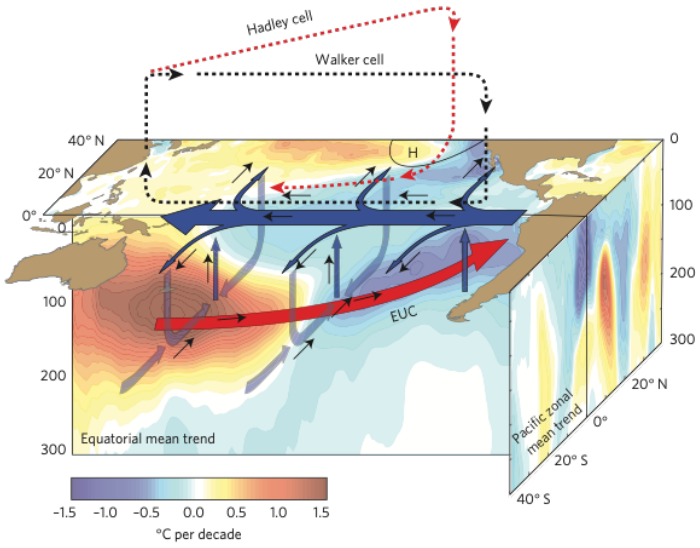

Figure 4. The upwelling at the equatorial Pacific is causing water to rise at both southern and Northern hemisphere. The current flows along the equator in an East-West direction, which refers to the EUC in this study (Braddock, 2018).

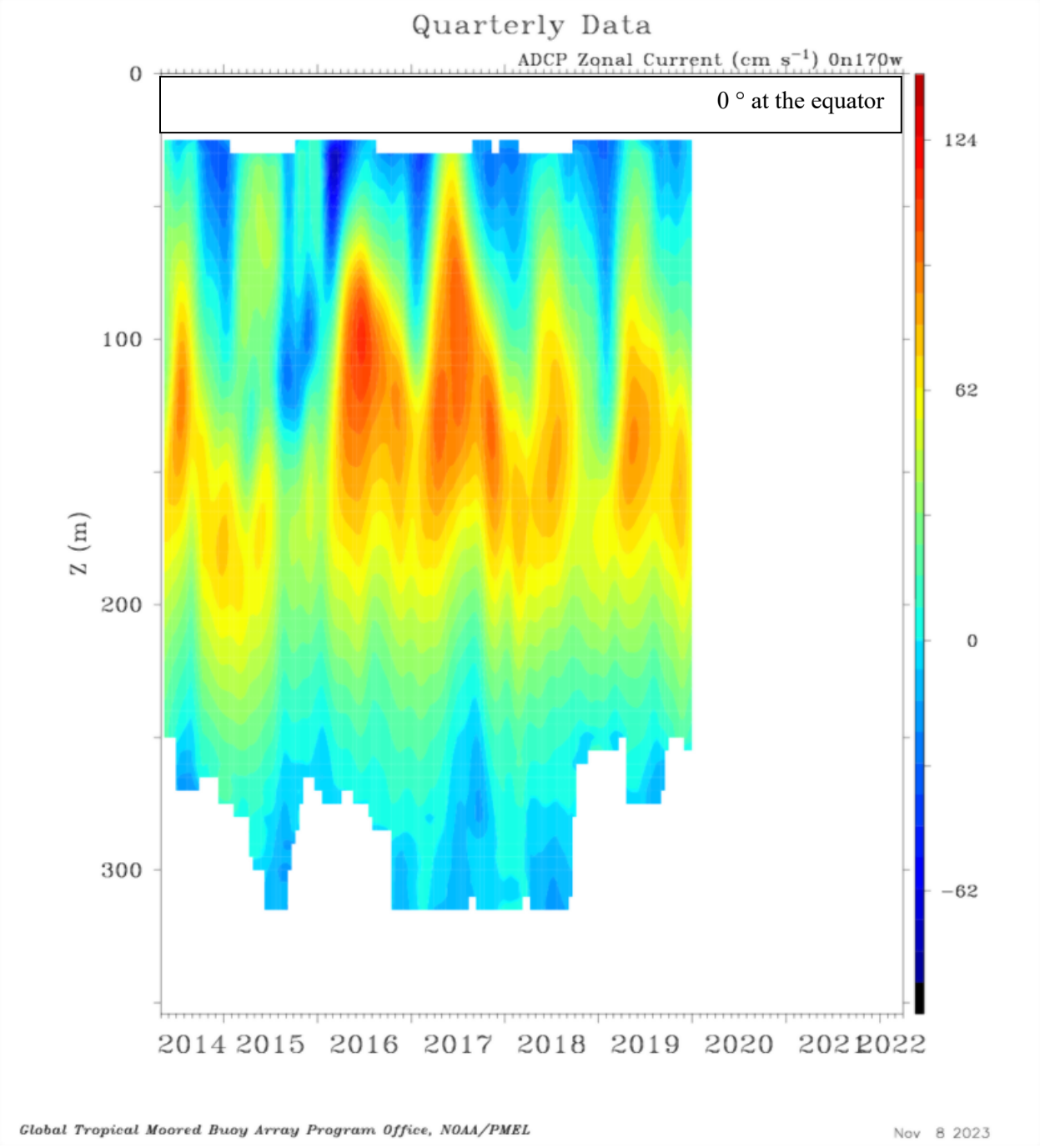

Figure 5. Monthly UADCP (UADCP is the East-West vector component of ocean current determined from ADCP observations, also referred to as the U or zonal component. Positive values are directed north.) data since 2019 (Global tropical moored Bouy Array, 2023).

The implication of this research is to investigate how the equatorial current changes during ENSO and predict how the current changes in a La Niña year. During the past El Niño year of 2016, EUC velocity was observed with a pattern. This study aims to justify this pattern using field data collected at the equator. It is expected that the zonal velocity will decrease and change direction from flowing east to west. Understanding the current structure is beneficial when studying the relationship between the equatorial current circulation and the temperature difference associated with ENSO.

Method:

Cruise TN427 carried by R/V Thomas G. Thompson setoff from port of Pago Pago in American Samoa (14.2771° S, 170.6844° W) on December 29th, 2023, traveling to 5°N and return to port of Pago Pago on January 10th, 2024. ADCP continued to operate during the entire cruise regardless of cruising speed. However, only data between 2°S to 2°N will be used in this study because the EUC is a narrow current flowing from west to east.

The topic of this paper is to is to compare 3 sets of ADCP data - one during the tail end of a La Niña period, the other near the peak of an El Niño, and the last one from TN413 cruise in March 2023. The expected work will involve obtaining current velocity data and plotting the current structure at each station. Therefore, this paper will compare the previous data to investigate the difference in current velocity brought about by change in phase of ENSO. Using the ADCP on R/V Thompson, current velocity readings at each station across the equator will be recorded,

while previous zonal ADCP data can be found on the Global Tropical Moored Buoy Array from NOAA. (Figure 5) Due to the long and narrow attributes of the EUC, its width is around 400 km, which is approximately 3.6° across the equator. The sampling range can then be narrowed down to a range of 2°N to 2°S. The cruise set off from Pago Pago, American Samoa, and reached the first two stations for seafloor mapping. Then the cruise proceeded to 5°S and traveled north to 5°N, making a round trip through the equator. The deployment of the ADCP will not be influenced by the condition and cruise speed (8 kts between each station and 0.5 kts while CTD sampling), meaning that the ADCP remains turned on throughout the process to produce continuous data. The specific ADCP models mounted on R/V Thompson are VM-ADCP: RDI Workhorse 75 kHz. Data from VM-ADCP will be collected through a Windows program from RDI instruments named Vessel-mounted data acquisition system (VMDAS). The program will be set up by a vessel technician; however, details including frequency require manual setup. To remove inevitable biases including ship movements and misalignment, necessary post-processing will be done on CODAS software. Finally, data analysis in different aspects can be conducted through MATLAB. The sources of the codes for data processing can be found on GitHub. (https://github.com/sebastianmenze/Processing-and-analysis-of-large-ADCP-datasets/blob/master/Processing%20and%20analysis%20of%20vessel%20mounted%20and%20lowered%20ADCP%20data.md). The ADCP data was post-processed by Cody Cruz using UHDAS+CODAS software from the University of Hawaii available at https://currents.soest.hawaii.edu/docs/adcp_doc/index.html (Firing et al. 2012). In addition to removing all periods beyond 2°S and 2°N to obtain a pure transect, threshold editing was applied to eliminate velocity values in bin ensembles with less than 80% good pings or greater than 500 mm/s error velocity magnitude. Phase correction was not warranted, but a final amplitude

correction of 1.006 was applied, resulting in median water-track calibration bias estimates of 1.0005 for amplitude and 0.0525° for phase. Because of ship stop during CTD casting, data during the stop will be removed for consitancy of produced graph. The ADCP data file will run through ADCP post-processing code in Jupyter notebooks writen by Cody Cruz, and the fully processed data (2024_os75nb_cleaned.nc) are available at https://github.com/GHOpenonic/equatorial-pacific-turbulent-mixing. (Cody, 2024, personal communication) The zonal current structure depth profile could be generated by code in Jupyter notebooks (https://drive.google.com/file/d/1CmYPK01Ij7HLt-L2Li8u4xbkbtrz_AKX/view?usp=sharing). The code will readin fully processed data and produce a graph. The bottom part of the code will calculate the transport of the EUC in m^3/s.

Equation (1)

$$Q = (H2 - H1) \times ((D2 - D1) \times 111000 \frac{m}{degree}) \times V_{mean} \quad (1)$$

A algorithm is applied to locate and calculate EUC specifically. Since EUC flows in the opposite direction to surface current, only current flowing towards east (positive) will be used for calculation. The variable Q represents zonal transport of EUC. It is related to the area of the cross section and maximum velocity. H2 and H1 are the maximum and minimum depth where the current velocity value is above zero. Since the EUC is shallower at the eastern Pacific and deeper at the western Pacific, the depth of EUC changes. However, the thickness of EUC should be equivalent at different locations. D2 and D1 are degrees in Latitude where current velocity value is above zero, multiplying the number by 111000 $\frac{m}{degree}$ to calculate the width of the EUC. V_{mean} is the mean velocity of current above zero with the range of H2, H1 and D2, D1. The result will be presented in Sverdrup (Sv) and 1 Sv is equivalent to 1 million cubic meters per second.

Result:

EUC is located at a specific location in the east-west cross section. Thus, a red square is applied to locate EUC and limit the range where maximum velocity of EUC is found. The Red square limits the depth and longitude parameters in equation (1), which is from 100 m to 200 m and from -2° S to 2° N.

By using the equation (1), the calculated transport within the red square for TN413 is 32.70 Sv. The maximum velocity of EUC is 1.03 $\frac{m}{s}$ (Figure 6) while the maximum velocity for TN427 was 0.41 $\frac{m}{s}$. The transport during TN427 is calculated to be 1.96 Sv. (Figure 7) The transport of the second crossing two days later is 3.51 Sv and maximum velocity within the square was 0.59 $\frac{m}{s}$ (Figure 8) The equatorial undercurrent velocity from TN413 cruise is larger than any of the crossing from TN427 cruise (Table 1).

The EUC velocities between two crossings in January 2024 are different as well. The EUC velocity during the second crossing is larger than the first crossing even though the second crossing only happens two days after the first one. Besides, the current structure is slightly different based on the contour map. (Figure 7) (Figure 8) The core of the EUC shifted to the north by approximately 1 deg.

After acquiring EUC velocity data in 2023 and 2024, the data can be added to TOGA / TAO UADCP data base and analyze the relationship between EUC velocity and Niño index. (Figure 9) The EUC velocity is acquired through TOGA / TAO website. Each data point represents the average annual EUC velocity, and it is calculated by taking the average of the highest EUC velocity each month within that year. The Niño index is taken from NOAA National Weather Service Climate Prediction Center. Each number is the average of 12 months index. The EUC

velocity data from TN 413 cruise and TN427 cruise fill in the last two data points where the velocity of TN427 cruise is the average value between two crossings.

Table 1: EUC Transport, maximum velocity, Mean velocity, and Mean velocity of the velocity above zero within the selected red square. Data was collected in March 2023 (TN413), January 2024 (TN427).

EUC values	Transport (Sv)	Max velocity ($\frac{m}{s}$)	Mean velocity ($\frac{m}{s}$)	Mean velocity above zero ($\frac{m}{s}$)
TN413 (2023)	37.23	1.03	0.37	0.44
TN427 first (2024)	10.77	0.42	0.02	0.14
TN427 Second (2024)	14.78	0.59	0.04	0.23

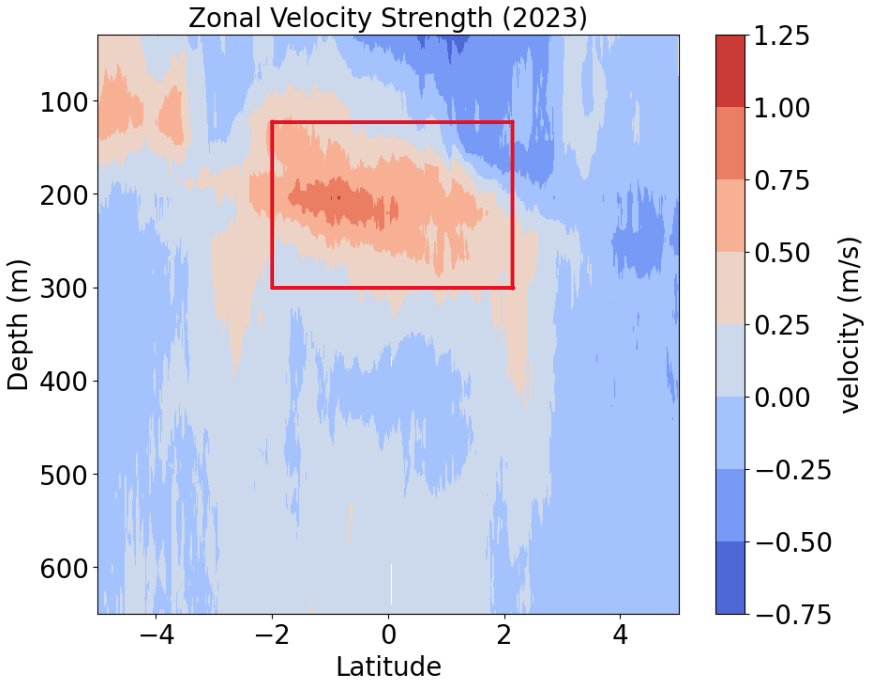

Figure 6. EUC current velocity data on Latitude during cruise TN413 from March 2023. Zonal velocity represents the East (positive) – West (negative) vector component of ocean current. Red square selects the region of EUC for calculation in equation (1).

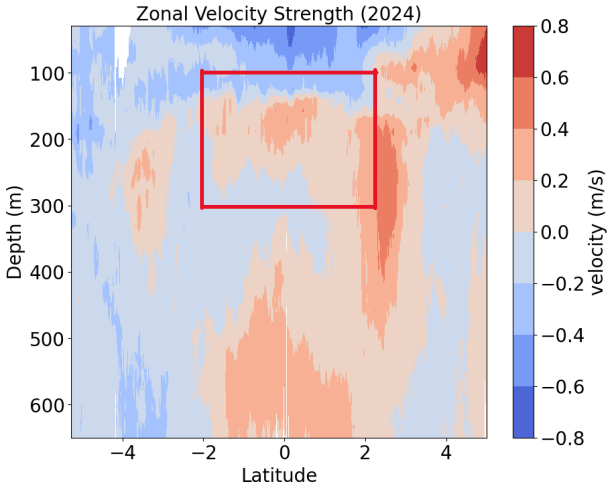

Figure 7. EUC current velocity data on Latitude during cruise TN427 from January 5, 2024. Zonal velocity represents the East (positive) – West (negative) vector component of ocean current. Red square selects the region of EUC for calculation in equation (1).

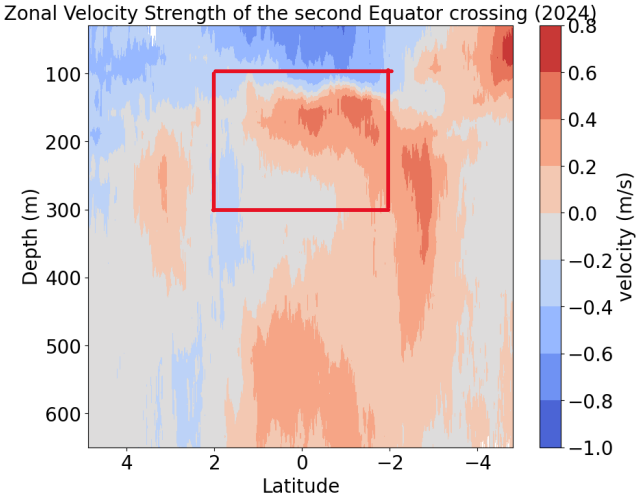

Figure 8. EUC current velocity data for the second crossing on Latitude during cruise TN427 from January 7, 2024. Zonal velocity represents the East (positive) – West (negative) vector component of ocean current. Red square selects the region of EUC for calculation in equation (1).

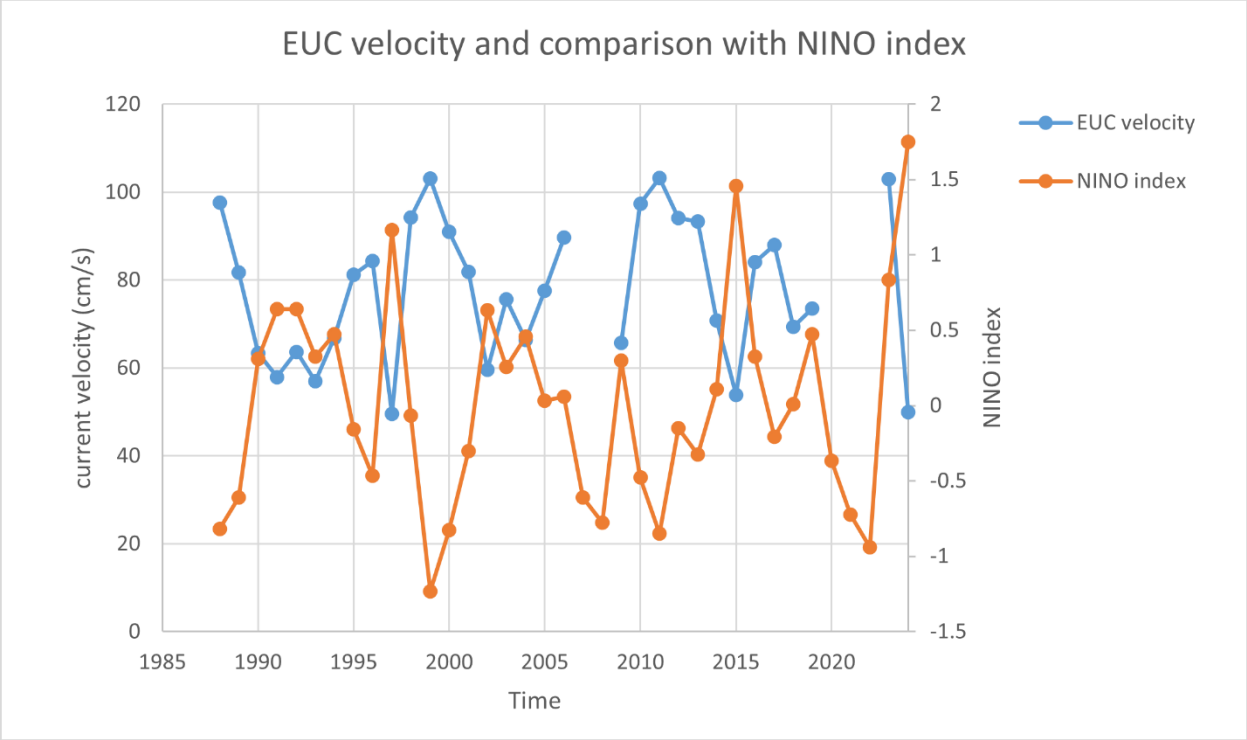

Figure 9. Comparison between average annual EUC velocity and average annual Niño index at Niño 3.4 region. The EUC velocity data is acquired from TOGA / TAO website and the available data gap between 2006 and 2009 and discontinued after 2019.

Discussion:

During the TN413 cruise in 2023, the maximum EUC velocity was 1.03 $\frac{m}{s}$, higher than the 0.41 $\frac{m}{s}$ and 0.59 $\frac{m}{s}$ during the TN427 cruise. Although the EUC direction did not reverse at the onset of El Niño, a noticeable decline in velocity was observed when comparing the maximum

velocities. An overall pattern from 1988 to 2024 (Figure 9) appears to show a correlation that EUC velocity is inversely proportional to the Niño index, with the EUC peak corresponding to the Niño index valley in 1999 and 2011. Although the EUC velocity never falls below 0, the variability of EUC velocity is still evident during the transition phase of the ENSO cycle. Hence, the last two data points of EUC velocity show a decreasing pattern while the Niño index is increasing. It is reasonable to predict that EUC velocity will continue to decrease below 0.5 $\frac{m}{s}$. The lowest average annual EUC velocity recorded by the TOGA/TAO database is 0.50 $\frac{m}{s}$ in 1997. There is a possibility that EUC velocity in 2024 and beyond will drop below this figure since the Niño index shows an increasing trend. As mentioned in the introduction, the strength of El Niño in 2024 is predicted to be equivalent to that in 2015-2016 and 1997-1998 (Climate Prediction Center Internet Team, 2023). According to the NOAA National Weather Service Climate Prediction Center, with an average annual Niño index of 1.46 in 2015 and 1.17 in 1997, the Niño index in 2024 (0.83) is expected to keep increasing, indicating a decreasing trend of EUC velocity. However, EUC velocity and transport could be influenced by seasonality. The integrated transport shows a longitudinal-seasonal variation from 1988 to 2007. Although the previous study only investigated from 160°W to 92°W, the seasonal variability follows a similar pattern and can be used to simulate the situation at 170°W. EUC transport reached its maximum value (49.75 Sv) around March and June, with the highest values occurring in March and April (Quintana et al., 2021). This pattern aligns with previous direct measurements of upper ocean currents (Johnson et al., 2002). Since the TN427 cruise sailed to 170°W in December and January, the EUC transport could be the lowest of the year; thus, further data are recommended for future prediction and conclusion. Note that the equation for calculating transport in Quintana's study differs from the one used in this study; therefore, the value of EUC transport in

this study should not be directly compared with Quintana's study. However, the overall pattern should be applicable to this study.

Conclusions:

The relationship between ENSO and EUC velocity is also critical when studying equatorial circulation. During El Niño, the EUC velocity is expected to be slower than the velocity during La Niña. In addition to that, the EUC velocity showed variation between two crossings of the equator during TN427 cruise in January 2024. Even though the second crossing only happened two days after the first crossing, the velocity increased by 40.5%. According to temperature reading of Niño 3.4 acquired from NOAA, the peak of El Niño was in January 2024 and started to decrease since then. However, the cause of this increase remains unsure. The seasonality brought by equatorial thermocline could lead to weekly variation while the weakening of El Niño could also lead to the slowing of EUC. Further study and data collection in the following month is suggested to determine the range of this seasonal variation.

Acknowledgement:

Here, I want to thank the University of Washington, School of Oceanography travel agency for planning this cruise.

Thanks to Professor Mark Warner, Rick Keil, Kathleen K Newell, François Ribalet, and Andrea S Ogston for providing lessons and experiences on the cruise.

Thanks to captain Eric Haroldson and the crews on R/V Thomas G. Thompson for providing us with a safe and wonderful journey.

Thanks to Cody Cruz, Kayla Robertson, and all students in Senior Thesis for the data and help on this research.

References:

Becker, E. et al. (2023). June 2023 ENSO update: El Niño is here. Retrieved from Climate.gov: https://www.climate.gov/news-features/blogs/enso/june-2023-enso-update-el-nino-here

Bjerknes, J. (1969). Atmospheric teleconnections from the Equatorial Pacific. Monthly Weather Review, 97(3), 163–172. https://doi.org/10.1175/1520-0493(1969)097

Climate Prediction Center Internet Team. (2023). EL NIÑO/SOUTHERN OSCILLATION (ENSO). Retrieved from Climate prediction center: https://www.cpc.ncep.noaa.gov/products/analysis_monitoring/enso_advisory/ensodisc.shtml

Johnson, G. C., & McPhaden, M. J. (2001). Equatorial Pacific Ocean Horizontal Velocity, Divergence, and Upwelling. Seattle, Washington: NOAA/Pacific Marine Environmental Laboratory.

McPhaden, M. J., et al. (2001). The El Niño–Southern Oscillation (ENSO) Observing System. Seattle: National Oceanic and Atmospheric Administration/Pacific Marine Environmental Laboratory.

Plimpton, P. E., & Foreman, H. (2004). Processing of Subsurface ADCP Data. Retrieved from NOAA Technical Memorandum OAR PMEL-125: https://tao.ndbc.noaa.gov/proj_overview/pubs/PDF/plimpton_adcp.pdf

Peng, (1998). Meridional Circulation Cells and the Source Waters of the Pacific. Retrieved from aami array: https://array.aami.org/amsonline/?request=get-document&issn=1520-0485&volume=028&issue=01&page=0062

Quay, P. D. (1983). Upwelling rates for the equatorial Pacific Ocean derived from the bomb 14C distribution. Journal of Marine Research.

Wang, Y. (2015). MOORED ACOUSTIC DOPPLER CURRENT PROFILER TIME SERIES. Retrieved from NOAA Technical Memorandum OAR-PMEL-146: https://www.pmel.noaa.gov/pubs/PDF/wang4307/wang4307.pdf

Wyrtki, K. (1981). An estimate of equatorial upwelling in the Pacific. Honolulu: Department of Oceanography, University of Hawaii.

Lin, Y.-S., et al. (2023). Effects of Equatorial Ocean Current Bias on Simulated El Niño Pattern in CMIP6 Models. Retrieved from AGU Advancing Earth and Space Sciences: https://doi.org/10.1029/2023GL102890

Firing, E., Hummon, J. M., & Chereskin, T. K. (2012). Improving the quality and accessibility of current profile measurements in the Southern Ocean. Oceanography, 25(3), 164–165, https://doi.org/10.5670/oceanog.2012.91.

Rosales Quintana, G. M., Marsh, R., & Icochea Salas, L. A. (2021). Interannual variability in contributions of the Equatorial Undercurrent (EUC) to Peruvian upwelling source water. Ocean Sci., 17, 1385–1402, https://doi.org/10.5194/os-17-1385-2021

Johnson, G. C., Sloyan, B. M., Kessler, W. S., & McTaggart, K. E. (2002). Direct measurements of upper ocean currents and water properties across the tropical Pacific during the 1990s. Prog. Oceanogr., 52, 31–61, https://doi.org/10.1016/S0079-6611(02)00021-6.

Cromwell, T., Montgomery, R., & Stroup, E. (1954). Equatorial Undercurrent in Pacific Ocean Revealed by New Methods. Science, 119, 648–649, https://doi.org/10.1126/science.119.3097.648.

Knauss, J. A. (1959). Measurements of the Cromwell current. Deep-Sea Res., 6, 265–286, https://doi.org/10.1016/0146-6313(59)90086-3.

McPhaden, M. J. (1999). Genesis and Evolution of the 1997–98 El Niño. Science, 283, 950–954, https://doi.org/10.1126/science.283.5404.950.

Firing, E., J.M. Hummon, and T.K. Chereskin. 2012. Improving the quality and accessibility of current profile measurements in the Southern Ocean. *Oceanography* 25(3):164–165, https://doi.org/10.5670/oceanog.2012.91.

Rosales Quintana, G. M., Marsh, R., & Icochea Salas, L. A. (2021). Interannual variability in contributions of the Equatorial Undercurrent (EUC) to Peruvian upwelling source water. *Ocean Sci.*, 17, 1385–1402. https://doi.org/10.5194/os-17-1385-2021

Johnson, G. C., Sloyan, B. M., Kessler, W. S., and McTaggart, K. E.: Direct measurements of upper ocean currents and water properties across the tropical Pacific during the 1990s, Prog. Oceanogr., 52, 31–61, https://doi.org/10.1016/S0079- 6611(02)00021-6, 2002.

Cromwell, T., Montgomery, R., and Stroup, E.: Equatorial Undercurrent in Pacific Ocean Revealed by New Methods, Science, 119, 648–649, https://doi.org/10.1126/science .119.3097.648, 1954.

Knauss, J. A.: Measurements of the Cromwell current, DeepSea Res. (1953), 6, 265–286, https://doi.org/10.1016/0146- 6313(59)90086-3, 1959.

McPhaden, M. J.: Genesis and Evolution of the 1997–98 El Niño, Science, 283, 950–954, https://doi.org/10.1126/science .283.5404.950, 1999.

Gu DF, Philander SGH (1997) Interdecadal climate fluctuations that depend on exchanges between the tropics and extratropics. Science 275:805–807.

Izumo, Takeshi. (2005). The equatorial undercurrent, meridional overturning circulation, and their roles in mass and heat exchanges during El Niño events in the tropical Pacific. Ocean Dynamics. 55. 110-123. 10.1007/s10236-005-0115-1.

Appendices: